A Microstructured Laser With Modulated Period for Beam Control

Yibo Yang , Zheng Wang , Jie Sun, Xiuyan Sun, Pengfei Wang, Xuliang Zhou, Jiaoqing Pan ,
Yejin Zhang , and Yanmei Su

Abstract—In this paper, a microstructured laser with modulated periodic microstructures for beam control is proposed for the first time. Lasers using modulated periodic microstructures can emit beam with lower vertical divergence angle for the same number of microstructures. And lasers with specific period length can transmit beam in specific direction. These lasers emitting beams with different emission directions can be integrated into an array. And this array can be used directly as a transmitter chip of LiDAR. Both simulation and experimental results show that the modulated periodic microstructures can effectively reduce the vertical divergence angle. In the experiment, the lowest vertical divergence angle of 0.88° and a large angle sweep range of 41.5° have been obtained. A horizontal divergence angle of 4.3° is achieved with the taper structure. Typical optical power is 29 mW.

Index Terms—Modulated period, periodic microstructures, laser array, vertical divergence angle.

I. INTRODUCTION

LIGHT detection and ranging (LiDAR) is broadly used in the automatic pilot system and the remote sensing [1], [2]. So far, several types of LiDAR are developed by the researchers, such as mechanical LiDAR [3], micro-electromechanical system (MEMS) LiDAR [4], flash LiDAR [5], and optical phased array (OPA) LiDAR [6]. However, these types of LiDAR have different limitations in the application. The complex scanning structure makes mechanical LiDAR expensive and vulnerable. The MEMS LiDAR has a complex optical path but a small scanning range. The flash LiDAR has shortage in pixel precision. In addition, the OPA LiDAR has problems in light utilization efficiency and integration of light sources. Therefore, we need a new LiDAR with simple structure and low price. We hope to fabricate a laser array as a LiDAR emitter chip by ordinary process. And it can emit direction controllable beams without mechanical component.

Conventional semiconductor lasers have larger vertical divergence angles (about 40°) and cannot be directly used for LiDAR. Although researchers reported some technologies for reducing the divergence angle, such as coupled waveguide [7], asymmetric waveguide [8], coupled large optical cavity [9], ridge waveguide [10], modified Bragg-like waveguide [11], super large optical cavity [12], and hybrid extended-distributed Bragg reflector [13], the vertical divergence angle is still difficult to be less than 10°. In order to solve this problem, microstructure is designed to control the direction angle and lower the vertical divergence angle. Yejin Zhang *et al.* have proposed a slotted single-mode laser with directional angle of 54.6° and a vertical divergence angle of 1.7° [14]. Xuefan Yin *et al.* have indicated that the topological defect guides unidirectional resonances to change direction of the beam emission [15]. Ahmed M. A. Hassan *et al.* have fabricated a vertical cavity surface-emitting laser with surface slots, and a very low divergence angle is achieved in specific direction [16]. Yanmei Su *et al.* have reported a direction tunable microstructured laser array with vertical divergence angles ranging from 1.3° to 3.5° [17]. However, as a lidar emitting chip, its performance characteristics may still be improved, particularly in terms of divergence angles and optical output power.

For the first time, modulated periodic microstructures are employed to lower the divergence angle of laser in this paper. This modulation methods allows to achieve a lower vertical divergence angle for the same number of microstructures. Meanwhile, it can change the direction of the beam emission. During the experiment, the emission direction of the beam changes from 69° (period of 8 μm) to 27.5° (period of 18 μm). The vertical divergence angles range from 0.88° to 2.59° and the horizontal divergence angles is around 4.3°. In addition, 29 mW optical power output is obtained.

II. DEVICE STRUCTURE

The ridge waveguide lasers are manufactured by III-V epitaxial wafer, as shown in Table I [17]. The wavelength of the laser is 1550 nm. Microstructures are etched into the ridge waveguide to adjust emission direction of beam and lower the vertical divergence angle.

The active region is composed of five pairs of quantum wells. Each pair of quantum well contains $[Al_{0.24}Ga]In_{0.71}As$ layer and $[Al_{0.44}Ga]In_{0.49}As$ layer. The active region is covered by 0.12 μm-thick separate confinement heterostructure (SCH)

TABLE I
ALGAINAS/INP MATERIAL STRUCTURE OF THE III-V EPITAXIAL WAFER

Name	Material	Thickness(μm)
P-contact	p- $Ga_{0.47}In_{0.53}As$	0.2
	p- $GaIn_{0.71}As_{0.62}P$	0.05
Cladding	p- InP	1.6
	p- $GaIn_{0.85}As_{0.33}P$	0.02
	p- InP	0.05
SCH	$[Al_{0.9}Ga]In_{0.53}As$	0.12
QW	$[Al_{0.24}Ga]In_{0.71}As\times5$	0.006
	$[Al_{0.44}Ga]In_{0.49}As\times6$	0.01
N-layer	$[Al_{0.9}Ga]In_{0.53}As$	0.13
N-contact	n- InP	0.8
Substrate	n- InP	

Fig. 1. (a) Structure diagram of the microstructured laser. (b) Schematic of the light emitting of the laser array.

layer. The 1.67 μm-thick cladding layer, and 0.25 μm-thick p-type contact layer is grown on the SCH layer as the waveguide layer.

In this work, fifteen microstructures are etched into the ridge waveguide to control the beam emitting direction and lower the vertical divergence angle. In addition, the arrangement of the microstructures makes a significant difference in managing the vertical divergence angle of the beams. A reasonable arrangement of the microstructures can achieve a lower vertical divergence angle in the same number of microstructures. The fifteen microstructures are split into three portions. And microstructures of each portion are arranged in varied period lengths. A 150 μm-thick laser array model is built for simulation. The period length and the size of the microstructures are optimized to strengthen the property of the lasers. Each laser can be individually designed to emit beam with low divergence angle in specific direction. These lasers with specific emission direction are integrated into an array chip to serve as the transmitter chip for the LiDAR.

As shown in Fig. 1(a), a taper structure is designed on the top to extend width of the ridge from 10 μm to 40 μm. And fifteen microstructures in three portions are arranged into different period length. The period lengths of the three parts are arranged in arithmetic progression of 3:2:1. The period length of the third part is the shortest of the three portions. In this work, the term 'period length' refers specifically to the period length of the third part. The X, Y and Z direction refer to the longitudinal, vertical, and horizontal direction, respectively. The cavity length of the laser is 2000 μm. Width, and depth of the microstructures are 1.1 μm and 1.4 μm, respectively.

As shown in Fig. 1(b), the difference in the period length of microstructures is 0.5 μm for two adjacent lasers. The period length is increased from 8 μm to 18 μm, and a total of 21 lasers are integrated into the array.

III. DEVICE CHARACTERISTICS AND ANALYSIS

The divergence angle of the far-field is positively correlated with the size of the light emitting area in the near-field. For the microstructured laser, a direct way to decrease the divergence angle of the far-field spot is to increase the number of microstructures. Nevertheless, it is shown that the energy loss from a microstructure in the waveguide is fixed [18]. Increasing
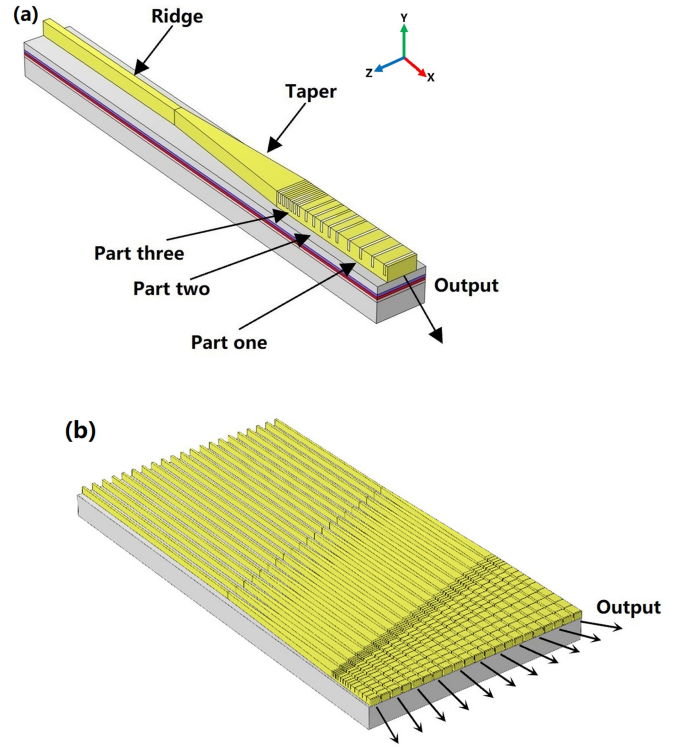
the number of microstructures infinitely will greatly affect the output power of the laser.

In addition, the relationship between the emission angle of the beam and the period length of the microstructures is given by (1) [19].

$$\sin\theta = \frac{m\lambda}{\Lambda}, \qquad (1)$$

where the Λ is the period length of the microstructures, the θ is diffraction angle, m is diffraction order and λ is the wavelength.

Let $\Lambda_n = n\Lambda$ and $m_n = nm$ to obtain (2):

$$\sin\theta = \frac{m_n\lambda}{\Lambda_n}, \quad n = 1, 2, 3\cdots, \qquad (2)$$

where the Λ_n is n times the period length of microstructures. And m_n is the nm order diffraction peak. According to (2), an integer multiple increase in the period length produces the diffraction peak of the beam at the same angle. The diffraction peak at this angle changes from the original m order to nm order.

In addition, the (3) is deduced from (1):

$$\sin\theta_{m+1} - \sin\theta_m = \frac{\lambda}{\Lambda}, \qquad (3)$$

where θ_{m+1} is the diffraction angle of $m+1$ order diffraction peak, and θ_m is the angle of m order. From (3), the difference between the angles of adjacent diffraction peaks is inversely proportional to the period length.

In this work, the arrangement of the three portions microstructures will produce the diffraction peak at same angle while
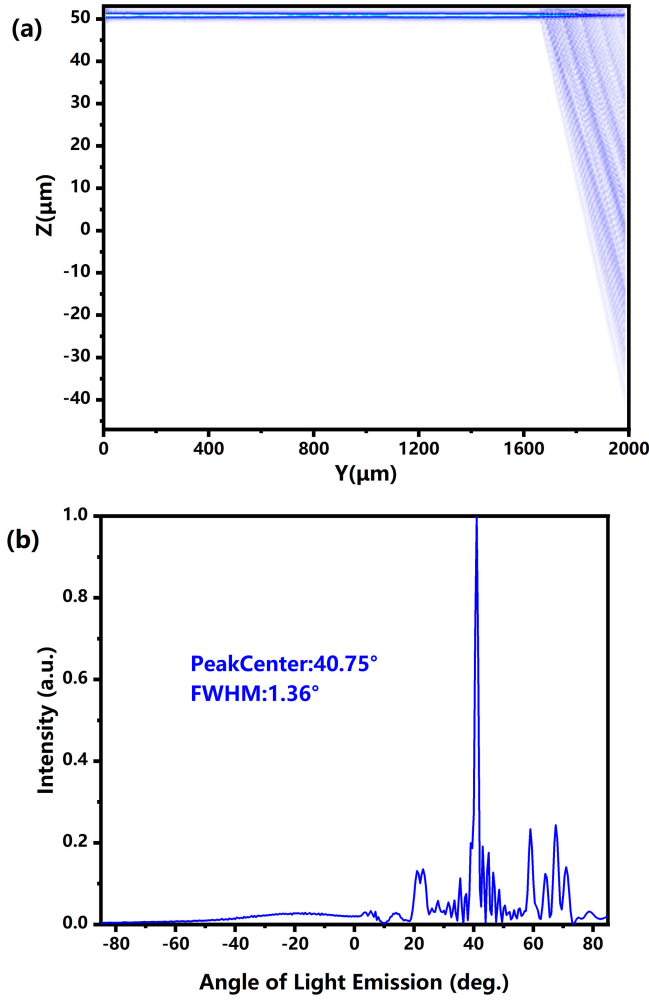
Fig. 2. (a) The optical transmission diagram of the longitudinal direction (XY cross section) and (b) the vertical far-field of microstructured laser with period length of 12 μm from simulation.

Fig. 3. The simulation results of (a) Vertical emission angles and (b) Vertical divergence angles.

expanding the near-field spot. This arrangement allows to obtain smaller vertical divergence angles for the same number of microstructures and avoids introducing additional energy losses.

The optical performances of twenty-one lasers with different period length are simulated by beam propagation method (BPM). The near-field is converted to the far-field by Fourier formula (4) [20].

$$I\left(\theta\right) = \left| \cos\theta \int_{-\infty}^{\infty} \tilde{u}\left(y\right) e^{i\frac{2\pi y}{\lambda}\sin\theta} dy \right|^2, \qquad (4)$$

where $\tilde{u}(y)$ is the near-field of the laser, and $I(\theta)$ is the relative intensity of far-field.

Fig. 2(a) shows the optical transmission diagram of longitudinal direction of the microstructured laser. The cavity length of the microstructured laser is 2000 μm, and the period length is 12 μm. The vertical far-field inferred by (4) from the near-field of the emitting surface is shown in Fig. 2(b). Under the influence of the modulated periodic microstructures, the emission direction of 40.75° is realized, and the vertical divergence angle as low as 1.36°.
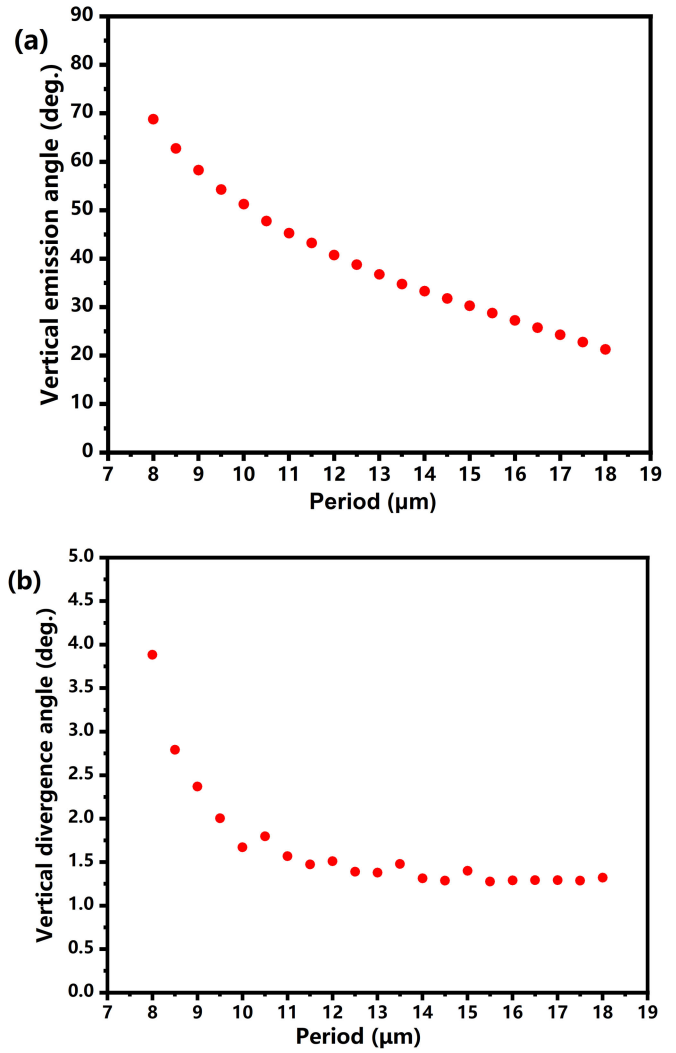
Fig. 3 shows the simulation results of the vertical emission angle and vertical divergence angle as a function of period length. In Fig. 3(a), as the period length increases from 8 μm to 18 μm, the vertical emission angle changes from 68.25° to 21.75°. And the vertical divergence angles of 21 lasers range from 3.36° to 1.27° as the period length changed.

According to the simulation results, two kinds of microstructured laser arrays with different arrangements of microstructures are fabricated to test performances. One is the lasers with uniform periodic microstructures and the other with the modulated periodic microstructures (Fig. 4).

The far-field characteristics of the microstructured lasers are tested by a scanning method at room temperature. The Fig. 5 shows the vertical far-field diagram of the lasers with different arrangements of microstructures at the period length of 12 μm. Under the influence of microstructures, the emission directions of both lasers are about 44°. However, for the same number of microstructures, the vertical divergence angle of the modulated periodic laser is as low as 0.88°. It is a quarter of the
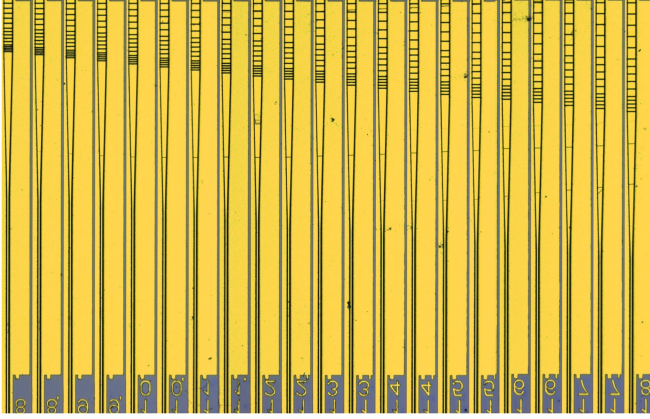
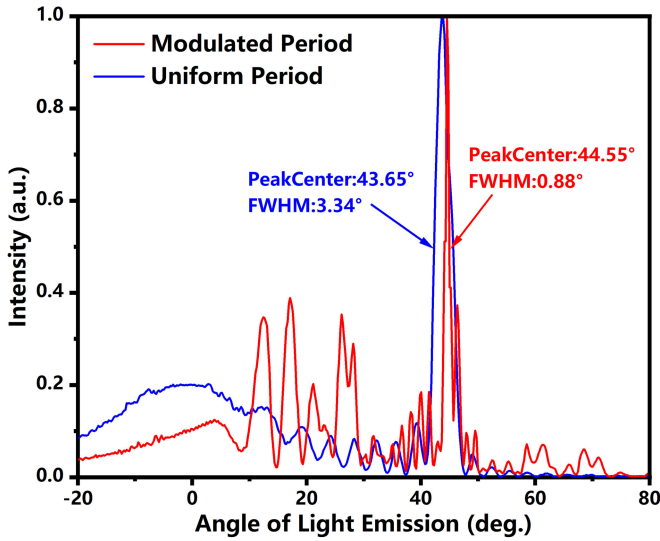Fig. 4. The photograph of the array chip with modulated periodic microstructured lasers.

Fig. 5. The vertical far-field diagram of the lasers with different arrangement of microstructures at the period length of 12 μm.
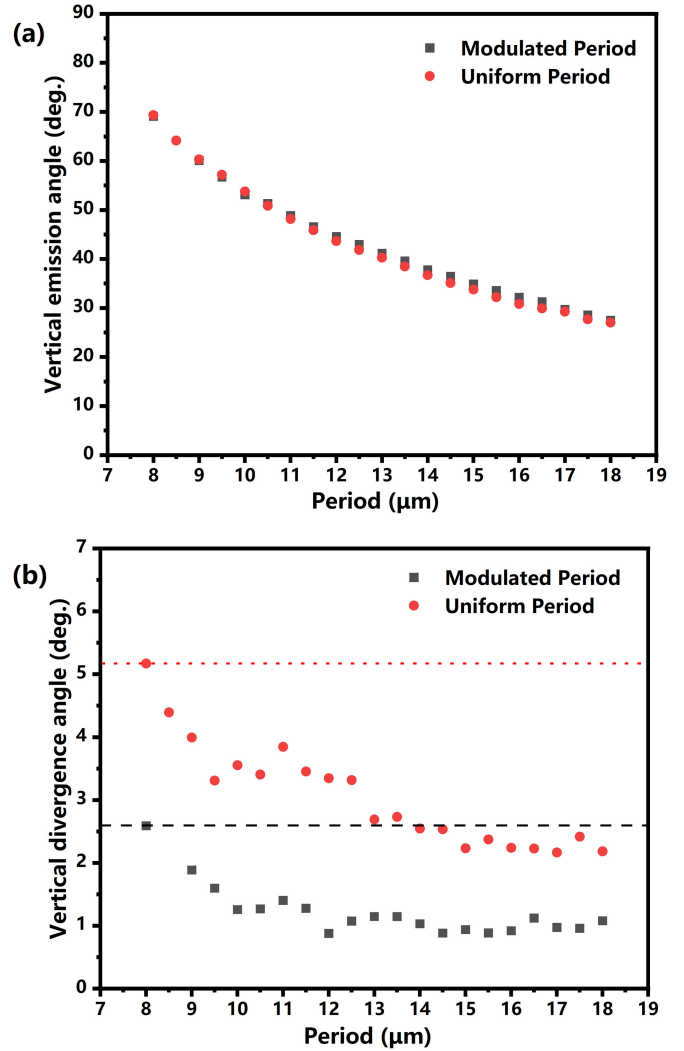

Fig. 6. The comparison of modulated periodic lasers and uniform periodic lasers of (a) the vertical emission angle and (b) Vertical divergence angle.

vertical divergence angle of the uniform periodic laser. That demonstrates the excellent performance of the modulated periodic microstructures in reducing the vertical divergence angle. According to (3), an increase in the period length brings the adjacent diffraction peaks close together. In the far-field diagram of modulated periodic laser, the lower intensity diffraction peaks between 10° and 30° are diffracted by microstructures with lager period lengths of fifteen microstructures. And the secondary diffraction peak robs the energy that originally leaks from the end face of the active region. Our next work is to seek for solution to reduce the divergence angle of the main peak while suppressing the secondary diffraction peaks and the energy loss from active region.

In Fig. 6, The vertical emission angle and vertical divergence angle of modulated periodic lasers are compared with uniform periodic lasers. As the period length increased from 8 μm to 18 μm, the emission angles of both lasers are correspondingly reduced from 69° to 27.5°. It means that the emission direction

of the beam is not related to the arrangement of microstructures. As shown in Fig. 6(b), the vertical divergence angle of the modulated periodic lasers is controlled between 2.58° and 0.88° with the period length changed from 8 μm to 18 μm. This result is much better than the lasers with uniform periodic microstructures. It indicates that the modulated periodic microstructures have an excellent effect on reducing the vertical divergence angle.

The output powers are measured by the Thorlab PM16-401 power meter at the room temperature. And the high-reflection coating is coated on the cavity surface of taper laser. Fig. 7 shows the typical light output power and voltage versus the continuous injection current of modulated periodic and uniform periodic lasers. For the uniform periodic laser, the typical power output and the threshold current is 24 mW and 180 mA, respectively. The typical output power and the threshold current of the modulated periodic laser is 29 mW and 200 mA, respectively. The arrangement of the microstructures does not affect the power-current-voltage characteristics of the lasers.
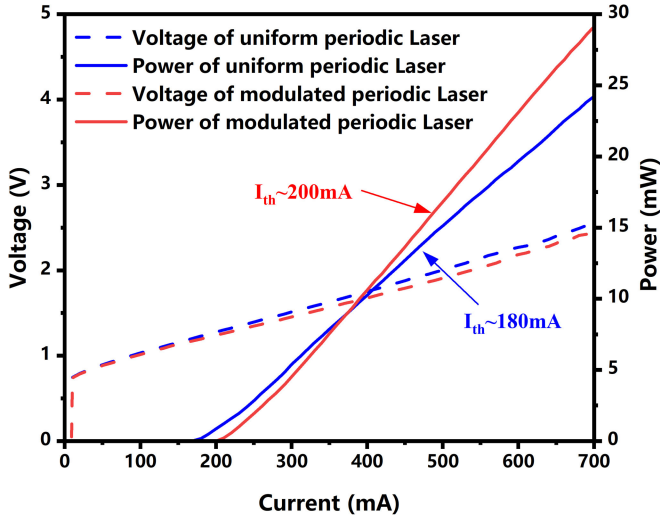
Fig. 7. Light output power and voltage versus the continuous injection current of modulated periodic and uniform periodic lasers.
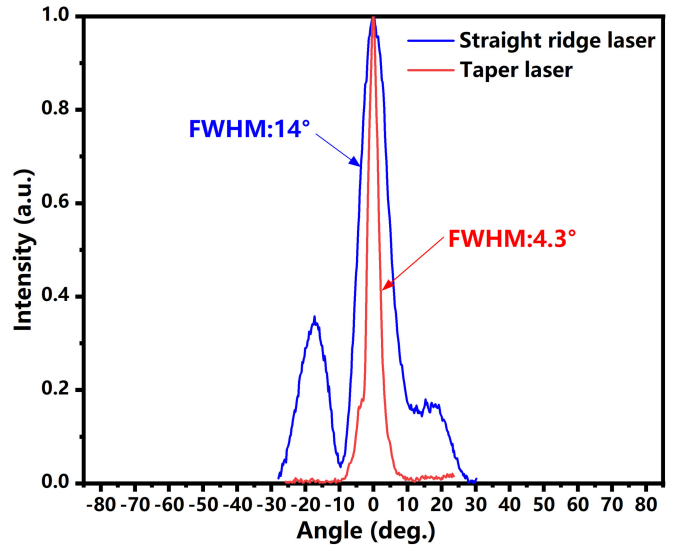

Fig. 9. Comparison of horizontal divergence angle between taper laser and straight ridge laser.
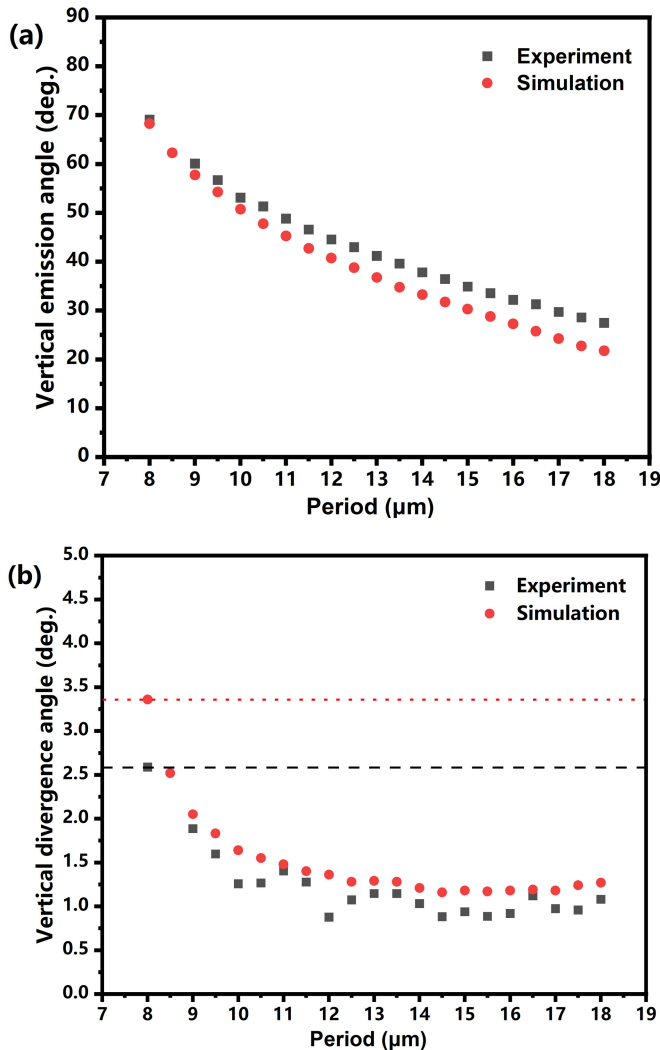

Fig. 8. Comparison of the simulation and the experimental results of (a) Vertical emission angles and (b) Vertical divergence angles.

And the difference between modulated periodic and uniform periodic laser stems from deviation in production process (like the homogeneity of high-reflection coating).

Fig. 8 shows the comparison of the simulation and the experimental results of the modulated periodic lasers. In Fig. 8(a), with the changes of period length, the emission angle of beams changes from 69° to 27.45°. And the vertical divergence angles of 21 lasers are shown in Fig. 8(b), which change from 2.59° to 0.88° with the period length changed. The experimental results basically conform to the trend of the simulation results.

In practical applications, a small horizontal divergence angle is desired. The taper structure is designed to lower the horizontal divergence angle. Fig. 9 shows the difference in horizontal divergence angle between taper laser and straight ridge laser. The ridge width and the cavity length of the straight ridge is 10 μm and 2000 μm, respectively. The horizontal divergence angle of the taper laser is 4.3°, which is one-third of the horizontal divergence angle of straight ridge laser. The taper structure has obvious superiority in reducing horizontal divergence angle.

IV. CONCLUSION

These experiments confirmed that the modulated periodic microstructures using arithmetic progression can effectively reduce the vertical divergence angle for the same number of microstructures. And the emission direction of the beams can be well controlled. In this work, based on the effective refractive index approximation and finite difference beam propagation method, the lasers with modulated periodic microstructures are simulated. And an array chip with modulated periodic lasers is fabricated to test. Both simulation and experimental results show the excellent performance of the modulated periodic microstructures in reducing the vertical divergence angle. A

vertical divergence angle as low as 0.88° and emission direction angles in the range of 27.5° to 69° are obtained in the experiment. Typical optical power is 29 mW with high-reflection coating. The laser with modulated periodic microstructures has a marvelous development prospect. In addition, the laser array requires only low-cost i-line projection photolithography during the whole fabrication process. The modulated periodic lasers can emit beams with a low vertical divergence angle. And each laser unit launches in a specified direction. Integrating different numbers of lasers with modulated periodic microstructures into an array as a scanning chip for LiDAR to meet different requirements. Combined with the driving circuit, fast scanning in different direction can be achieved.

REFERENCES

[1] R. A. Zahawi, J. P. Dandois, K. D. Holl, D. Nadwodny, J. L. Reid, and E. C. Ellis, "Using lightweight unmanned aerial vehicles to monitor tropical forest recovery," *Biol. Conservation*, vol. 186, pp. 287–295, Jun. 2015, doi: 10.1016/j.biocon.2015.03.031.

[2] D. Cunningham, S. Grebby, K. Tansey, A. Gosar, and V. Kastelic, "Application of airborne LiDAR to mapping seismogenic faults in forested mountainous terrain, southeastern Alps, Alovenia," *Geophys. Res. Lett.*, vol. 33, no. 20, 2006, Art. no. L20308, doi: 10.1029/2006GL027014.

[3] V. Freudenthaler, "About the effects of polarising optics on LiDAR signals and the Δ 90 calibration," *Atmosph. Meas. Techn.*, vol. 9, no. 9, pp. 4181–4255, Aug. 2016, doi: 10.5194/amt-9-4181-2016.

[4] Q. Hu, C. Pedersen, and P. J. Rodrigo, "Eye-safe diode laser Doppler LiDAR with a MEMS beam-scanner," *Opt. Exp.*, vol. 24, no. 3, pp. 1934–1942, Feb. 2016, doi: 10.1364/OE.24.001934.

[5] H. V. Duong, M. A. Lefsky, T. Ramond, and C. Weimer, "The electronically steerable flash LiDAR: A full waveform scanning system for topographic and ecosystem structure applications," *ITGRS*, vol. 50, no. 11, pp. 4809–4820, Nov. 2012, doi: 10.1109/TGRS.2012.2193588.

[6] T. Komljenovic, R. Helkey, L. Coldren, and J. E. Bowers, "Sparse aperiodic arrays for optical beam forming and LiDAR," *Opt. Exp.*, vol. 25, no. 3, pp. 2511–2528, Feb. 2017, doi: 10.1364/OE.25.002511.

[7] J. N. Walpole *et al.*, "Slab-coupled 1.3-mu m semiconductor laser with single-spatial large-diameter mode," *IPTL*, vol. 14, no. 6, pp. 756–758, Jun. 2002, doi: 10.1109/LPT.2002.1003083.

[8] V. P. Kalosha, K. Posilovic, and D. Bimberg, "Lateral-longitudinal modes of high-power inhomogeneous waveguide lasers," *IEEE J. Quantum Electron.*, vol. 48, no. 2, pp. 123–128, Feb. 2012, doi: 10.1109/JQE.2011.2169651.

[9] N. Y. Gordeev *et al.*, "Transverse single-mode edge-emitting lasers based on coupled waveguides," *Opt. Lett.*, vol. 40, no. 9, pp. 2150–2152, May 2015, doi: 10.1364/OL.40.002150.

[10] M. J. Miah *et al.*, "1.9 W continuous-wave single transverse mode emission from 1060 nm edge-emitting lasers with vertically extended lasing area," *Appl. Phys. Lett.*, vol. 105, no. 15, Oct. 2014, Art. no. 151105, doi: 10.1063/1.4898010.

[11] L. Wang *et al.*, "High-power ultralow divergence edge-emitting diode laser with circular beam," *IEEE J. Sel. Topics Quantum Electron.*, vol. 21, no. 6, pp. 343–351, Nov./Dec. 2015, doi: 10.1109/JSTQE.2015.2420669.

[12] S. P. Abbasi and M. H. Mandieh, "Improvement of AlGaInAs/AlGaAs laser diode electro-optics characteristics by graded refractive index profile broadened waveguide," *Opt. Laser Technol.*, vol. 116, pp. 155–161, Aug. 2019, doi: 10.1016/j.optlastec.2019.03.020.

[13] C. Xiang, P. A. Morton, and J. E. Bowers, "Ultra-narrow linewidth laser based on a semiconductor gain chip and extended Si_3N_4 Bragg grating," *Opt. Lett.*, vol. 44, no. 15, pp. 3825–3828, Aug. 2019, doi: 10.1364/OL.44.003825.

[14] Y. J. Zhang *et al.*, "Inclined emitting slotted single-mode laser with 1.7 degrees vertical divergence angle for PIC applications," *Opt. Lett.*, vol. 43, no. 1, pp. 86–89, Jan. 2018, doi: 10.1364/OL.43.000086.

[15] X. F. Yin, J. C. Jin, M. Soljacic, C. Peng, and B. Zhen, "Observation of topologically enabled unidirectional guided resonances," *Nature*, vol. 580, no. 7804, pp. 467–471, Apr. 2020, doi: 10.1038/s41586-020-2181-4.

[16] A. M. A. Hassan, X. D. Gu, M. Nakahama, S. Shinada, M. Ahmed, and F. Koyama, "High power surface grating slow-light VCSEL," *Appl. Phys. Exp.*, vol. 14, no. 9, Sep. 2021, Art. no. 092006, doi: 10.35848/1882-0786/ac1de7.

[17] Y. M. Su *et al.*, "Emitting direction tunable slotted laser array for LiDAR applications," *Opt. Commun.*, vol. 462, May 2020, Art. no. 125277, doi: 10.1016/j.optcom.2020.125277.

[18] Q. Y. Lu *et al.*, "Analysis of slot characteristics in slotted single-mode semiconductor lasers using the 2-D scattering matrix method," *IEEE Photon. Technol. Lett.*, vol. 18, no. 24, pp. 2605–2607, Dec. 2006, doi: 10.1109/lpt.2006.887328.

[19] A. Ghatak, "Fraunhofer diffraction: I," in *Optics*, 6th ed., X. Zhang, X. Tang, and H. Zhang, Eds., Beijing, China: Tsinghua Univ. Press, 2019.

[20] H. C. Casey, Jr., M. B. Panish, and J. L. Merz, "Beam divergence of the emission from double-heterostructure injection lasers," *J. Appl. Phys.*, vol. 44, pp. 5470–5475, 1973, doi: 10.1063/1.1662178.